7.1 MORPHOLOGY AND MECHANICAL PROPERTIES OF COMMERCIAL $M_{n+1}AX_n$ PHASES UNDER NEUTRON IRRADIATION — C.Ang, A. Campbell, N. Cetiner, C. Silva, C. Shih, Y. Katoh, S.J. Zinkle (Oak Ridge National Laboratory, USA), T. Toyama, T. Shikama (Tohoku University, Japan)

OBJECTIVE

$M_{n+1}AX_n$ (MAX) phases are potential candidates for future nuclear applications due to their potentially unique radiation tolerance. The present work evaluates the effects of neutron irradiation on selected MAX phase materials at moderate (~2, 6 and 10 dpa) radiation doses.

SUMMARY

MAX phases ternary nitrides and carbides were previously characterized (DOE/ER-0313/55). These nominally "Ti_3SiC_2" and "Ti_2AlC" compositions were irradiated to 2 x 10^{25} n/m^2 (E > 0.1 MeV), ~ 2 dpa (SiC). Both materials (referred to as Ti-Si-C and Ti-Al-C) had impurities, including ~6 wt% uncarburized $Al_{11}Ti_5$ and $TiSi_2$ This report covers specimens in Capsules 1, 4 and 7 irradiated at target temperatures of 400, 700 and 1000°C. Mechanical properties of Ti-Al-C were severely degraded at low irradiation temperatures due to grain boundary microcracks attributed to anisotropic swelling. Ti-Si-C consistently maintained moderate strength. Electrical resistivity suggested that metallic Si and Al layers were disrupted at 400°C by point defect accumulation, which recovered in the irradiation temperature interval 400 to 700°C. Ti-Al-C mechanical properties recovered at ~700°C. Young's modulus appeared unaffected. Swelling was more consistent in Ti-Si-C. Conclusions from XRD data were limited, particularly for Ti-Al-C material.

PROGRESS AND STATUS

Introduction

The promise of hybrid metal-ceramic materials from $M_{n+1}AX_n$ (MAX) phases is of interest to engineering ceramics, particularly given the attractive reports of a reversible slip-based deformation mechanism, implying that catastrophic failure associated with brittle fracture could be mitigated or nullified.[1] The lamellar atomic structure of metallic "A-layer" metal atoms alternating between crystalline "MX" ceramic unit cells yield good machinability, thermal and electrical conductivity in addition to high temperature strength and possible ductility. The alternating layers represent an ultra-high density of nanoscale interfaces that may function as natural sinks for mitigating defect accumulation that is responsible for degradation of materials under irradiation.[2] Both Ti-Al-C and Ti-Si-C specimens were irradiated at the High Flux Isotope Reactor (HFIR) during 2013. After a period of cooling, investigation of mechanical properties (swelling, elastic modulus, fracture strength), morphology (microcracking, changes in interfaces) and microstructure (irradiation-induced defects, lattice expansion, phase changes) commenced. The acquired materials were adequate as a first screening to assess whether these MAX phases were suitable for further development.

Experimental Procedures

For details, see DOE/ER-0313/55.

Results

<u>Irradiation temperature</u>
The irradiation temperature was determined by SiC temperature monitors (TMs) inserted in the capsules. The technique identified the change in instantaneous coefficient of thermal expansion (CTE) once heating annealed the irradiation induced defects.[3] The SiC TMs in Capsules 1, 4 and 7 respectively reached irradiation temperatures 370°C (643K), 620°C (893K) and 640°C (910K). These temperatures were then correlated to individual specimens using thermal modeling using ANSYS 12.0. This can be seen in Figure 1.

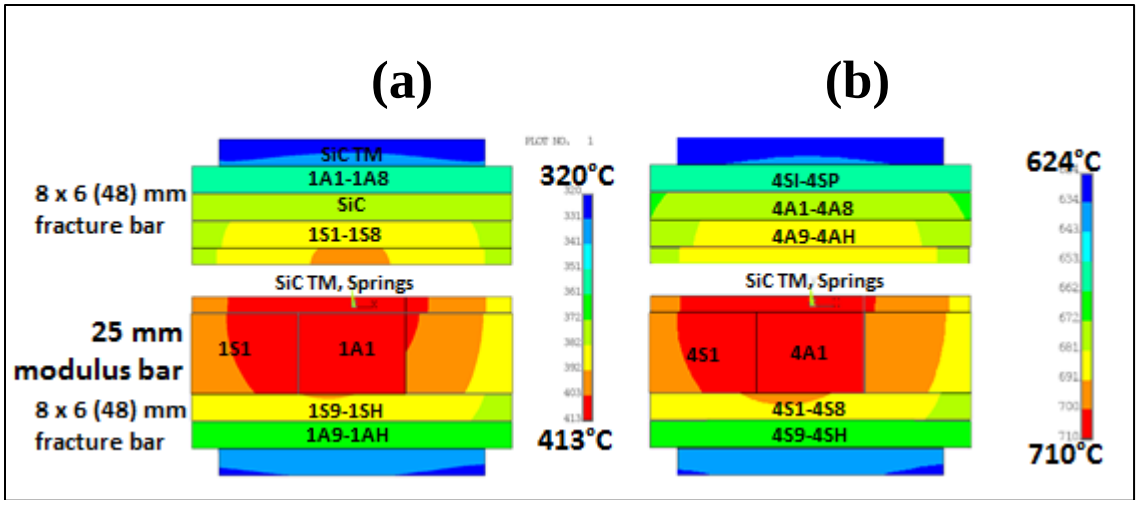

Figure 1. Specimen configuration for **(a)** Capsule 1 and **(b)** Capsule 4. Overlayed is a 2D thermal modelling showing respective temperature distributions as viewed from the end of the capsule where the modulus bars were inserted.

For convenience, the same color map was used for both Capsules 4 and 7. Since the intervals in color mapping in Figure 1 were ~10°C, and the TMs are deconvoluted to ±15°C, a value of ±25°C was used as the range of possible error for the irradiation temperature in parenthesis.

Scanning electron microscopy (SEM)

Figure 2(a) and (b) show the morphology of the as-received material after machining, polished to 40 nm OP-S. A Back-Scatter Electron (BSE) detector was used to show Z-atomic contrast to assist limited phase identification. In (a), the Ti-Al-C grains were anisotropic and up to 50 µm in length due to preferential a-axis growth. Due to an incomplete reaction, material contained an estimated Ti_3AlC_2 (43 wt%) Ti_2AlC (34 wt%) $Ti_5Al_2C_3$ (16 wt%) by XRD. These phases are indistinguishable by SEM, however, attempts to select grains using Electron Back Scatter Diffraction (EBSD) are currently in progress. In Figure 2(b), the Ti-Si-C shows an identical morphology but has a finer grain size and dispersed intergranular particles and TiC is observed as the brighter, equiaxed, dispersed intergranular particles. An alumina intergranular phase was also noted in the report, and can be seen by the bright contrast and low contact angle. This is likely from contamination of milling media. In both materials, an intermetallic Ti_5Al_{11} (6.4 wt%) or $TiSi_2$ (5.7 wt%) phase was observed. For further details, see DOE/ER-0313/55.

Recovered specimens from Capsules 1, 4 and 7 were polished to 1 µm finish. Figure 2(c) shows the neutron irradiated Ti-Al-C material, with an irradiation temperature (see Figure 1(a)) of 401(25)°C. Extensive transgranular and minor intergranular cracking through the material was observed. Figure 2(d) shows that Ti-Si-C irradiated at a temperature of 435(25)°C showed no differences in morphology. Microscopy is continuing.

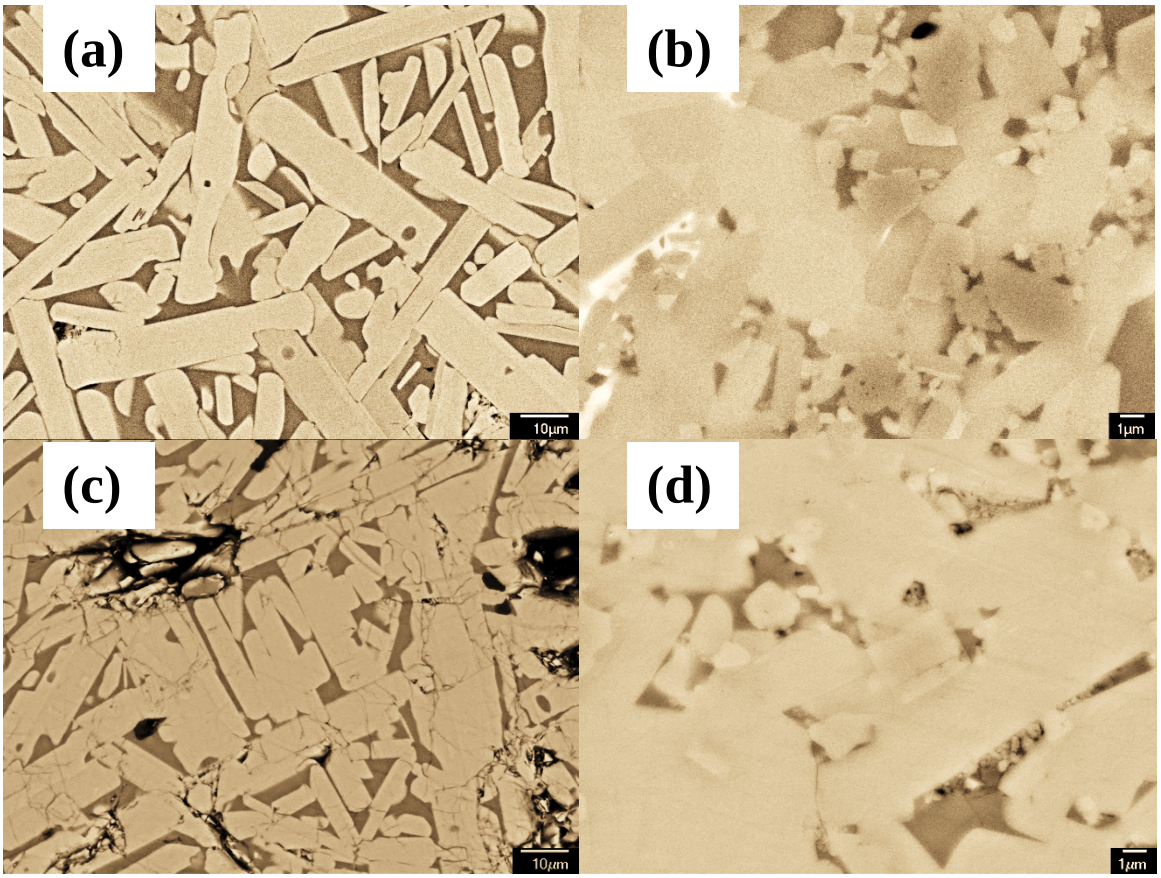

Figure 2. (a) SEM image of as-machined and polished Ti-Al-C (b) Ti-Si-C. Post-irradiation SEM images of (c) Ti-Al-C and (d) Ti-Si-C.

Swelling and density

Figure 3(a) shows the volumetric swelling measured from the modulus bars. It can be deduced that Ti-Si-C swelling of 0.8%, 0.9% and 1.5% for Capsules 1, 4 and 7 is more consistent than Ti-Al-C, which experienced variations in volumetric swelling from 4.0%, -0.4% and 1.65% at the respective temperatures. In Ti-Al-C material, the increase of 2% swelling from Capsule 4 (705°C) to Capsule 7 (725°C) may be caused by errors in swelling measurement or phase transformation during irradiation. Figure 3(b) shows the density measurements of the samples, which were in agreement with the swelling in Figure 3(a). Archimedes density on specimens using ASTM B962 used a proprietary 3M Fluorinet Liquid FC-43 as the suspension and immersion medium. The only anomalous result was Ti-Al-C Capsule 1, where the increase in volumetric swelling is accompanied by an *increase* in density, followed by a return to as-received values.

In Ti-Si-C, the trend of decreasing density was consistent with increasing volumetric swelling. Interestingly, Figure 3 shows that at ~700°C irradiation temperature, both materials show a decrease in density and increase in swelling. Further density measurements are to follow.

Phase analysis (XRD)

Rietveld analysis of XRD data was conducted using GSAS™ and CrystalDiffract™ Suite. Crystallite size and strain were calculated by Williamson-Hall method. The refinement was adequate for Ti-Si-C. The major phase of Ti_3SiC_2 (ICSD-180419) was identified in all samples, with a minor phase identified as TiC (ICSD-5910091). There were minor peaks in the XRD patterns that were not properly identified. The quantity of Ti_3SiC_2 decreases after irradiation by ~10 wt% relative to the TiC phase. The TiC unit cell expands isotropically; in Ti_3SiC_2 an expansion of the crystal structure occurs via a proportional elongation

of the c-axis by 1.0% and corresponding shrinkage of the a-axis. At higher irradiation temperatures, the TiC content and lattice parameters of both phases return to as received values.

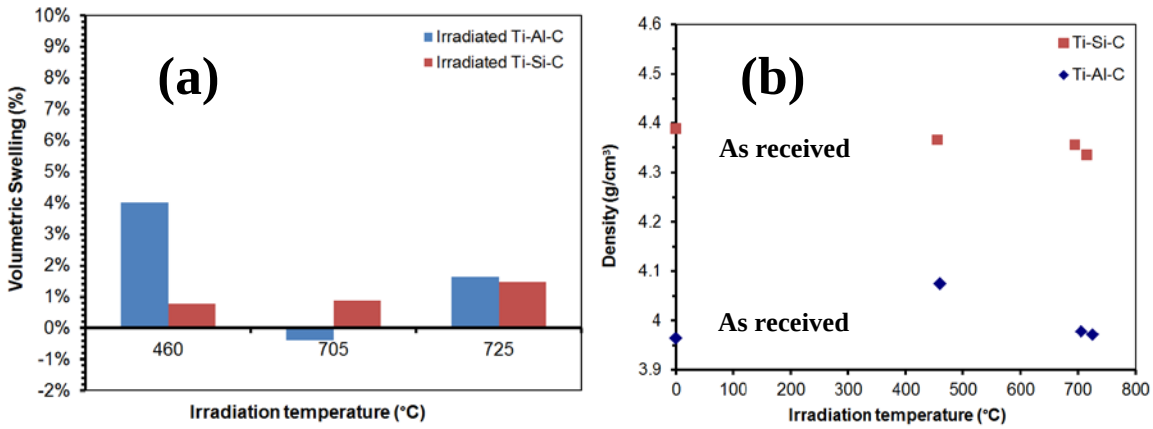

Figure 3. (a) Volumetric swelling on MAX phase materials compared to specimen original dimensions **(b)** Density of specimens after irradiation (compared to "As received").

The analysis of Ti-Al-C material should be considered qualitative. Ti_2AlC and Ti_3AlC_2 possess identical space groups, resulting in peak overlap. By selecting to model with Ti_3AlC_2, it obviously ignores Ti_2AlC and $Ti_5Al_2C_3$ in the pattern fitting. It has been reported that TiC was found upon decomposition of Ti_3AlC_2 and Ti_2AlC materials under low neutron doses, indicating that the absence of Al layer results in de-twinning to a Ti-C material; additional work by Patel et al suggests that a Ti_3C_2 structure forms but no ICSD database file exists to fit a Rietveld model.[4, 5] The relative weight of Ti_3AlC_2 (or more precisely the "MAX phases") decreases by 5 wt% after irradiation and TiC content increased. An expansion of the crystal structure occurs via a proportional elongation of the c-axis by 1.0% and shrinkage of the a-axis after irradiation in Capsule 1. This is significantly less than ~1.7% reported by Tallman et al for Ti_3AlC_2 at a lower neutron dose of 0.1 dpa, but recall that Ti_2AlC c-axis expansion was ~1%[4]. Given the composition of the Ti-Al-C material, these values are reasonable. In cross-referencing Figure 3(a), this indicates the majority of the swelling is from microcracks. In both materials, low temperature irradiation yielded a drop in crystallite size, MAX phase content and increase in microstrain; at higher irradiation temperatures, microstrain values decreased and MAX phase content increased.

<u>Electrical resistivity</u>

Electrical resistivity ($\times 10^{-7}$ Ωm) values for as-received materials were 4.8 and 2.7 for Ti-Al-C and Ti-Si-C respectively. Room temperature resistivity increased after irradiation in Capsule 1 to a high value of 56 for Ti-Al-C and 9.3 for Ti-Si-C. The results are plotted in Figure 4.

Since electrical conductivity is primarily from the metal "A" layers in the MAX phase, this is suggestive of defects in the Si/Al layer. When compared to phase pure materials from Drexel University, it appears from Figure 4(a) that for Ti-Al-C, the 211 phase maintains electrical conductivity better than the 312 phase after irradiation.[4]

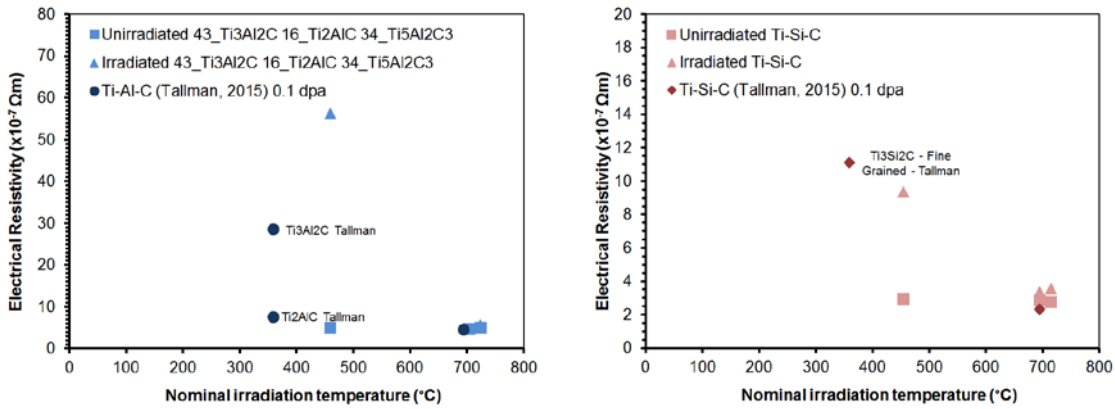

Figure 4. Electrical resistivity data for **(a)** Ti-Al-C material and **(b)** Ti-Si-C (nominally Ti_3SiC_2) compared with published data.[4] FG Ti_3SiC_2 is equivalent to ORNL Ti-Si-C.

Mechanical properties

The Dynamic Young's (E_y) modulus was measured for individual specimens. The average values across all as-machined specimens was 313.4(6.2) GPa for Ti-Si-C and 250.8(6.5) GPa for Ti-Al-C. The six specimens with their pre- and post-irradiation conditions are shown in Figure 5(a) and (b). The Capsule 1, 4 and 7 temperatures for the modulus bars were respectively 460(25), 705(25) and 725(25)°C. For the Ti-Al-C in Capsule 1, the E_y dropped from 241±3.2 GPa to 202±2.2 GPa. After irradiation in Capsule 4, the pre-irradiated value of 254 GPa matched the post-irradiation value of 257±1.0 GPa. With only a slight increase in irradiation temperature in Capsule 7, modulus abruptly decreased from 285 GPa to 214±0.2 GPa.

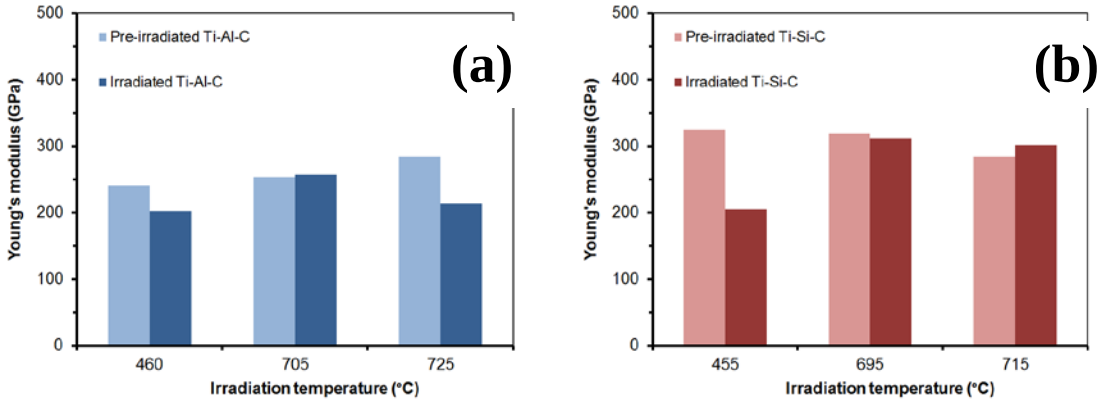

Figure 5. Elastic modulus individual 25 mm modulus bars of **(a)** Ti-Al-C **(b)** Ti-Si-C before and after irradiation at ~2 dpa.

In Ti-Si-C material (Figure 5(b)), irradiation in Capsule 1 reduced the modulus from 325 GPa to 205(6) GPa. In Capsule 4, the specimen appeared unaffected, with a pre-irradiated value of 319 GPa and 312(1) GPa. Finally, after Capsule 7 conditions, the modulus increased slightly from 285 GPa to 302(0.8) GPa.

Equibiaxial ring-on-ring fracture strength was measured according to ASTM C1499 using multipurpose square discs at room temperature. Table 1 shows the results. After irradiation in Capsule 1, Ti-Al-C tested at room temperature showed a loss of equibiaxial flexural strength as shown in Table 1, from 308(16) MPa on 31 specimens to 28(5) MPa based on the two selected specimens. Tests on single specimens recovered from Capsules 4 and 7 at the higher irradiation temperature shows that strength is maintained

at ~300 MPa. Ti-Si-C shows a small decrease in strength after irradiation in Capsule 1 and recovers to unirradiated values in Capsules 4 and 7.

Table 1. Room temperature ring-on-ring fracture strength after irradiation at 2 dpa.

Material/ID	Corrected irradiation T (°C)	F (N)	t (mm)	σ_f (MPa)
Ti-Si-C (31 tests)	As purchased	-	-	444.8 (29.5)
Ti-Si-C 1S7, 1S8	370+67 = 437(25)°C	115	0.484	302 (6.0)
Ti-Si-C 4S2	620+62 = 682(25)°C	128	0.511	302.1
Ti-Si-C 7S8	640+66 = 706(25)°C	171	0.572	322.2
Ti-Al-C (31 tests)	As purchased	-	-	307.8 (15.8)
Ti-Al-C 1A7,1A8	370+46 = 416(20)°C	12.0	0.511	28 (5.3)
Ti-Al-C 4AA	620+62 = 682(25)°C	121	0.497	302.5
Ti-Al-C 7AH	640+53 = 693(25)°C	150	0.558	297.0

The key result was that the microcracking observed in Ti-Al-C at Capsule 1 results in a substantial loss of strength since cracking prevents continuous load transfer, apart from mechanical interlocking between anisotropic grains.

Conclusions

$M_{n+1}AX_n$ (MAX) phase materials exhibited reduced electrical conductivity and materials properties after irradiation, although defects responsible for these effects appeared to balance against dynamic interstitial migration between 460°C and 700°C. In Ti-Al-C, low temperature irradiation leads to accumulation of point defects, which appear to be removal of Al on the A-layer and reduction in electrical conductivity. This results in smaller crystallite size and increased microstrain, calculated to lead to ~ 1% anisotropic elongation of the unit cell c-axis, resulting in grain boundary cracks that contribute to substantial swelling and absence of mechanical strength. At higher irradiation temperatures, recovery of mechanical properties occurs. In Ti-Si-C, the same process appears to displace the Si on the A-layers, leading to reduced electrical conductivity, increased microstrain and reduced crystallite size, but no microcracking is observed. A minor reduction in strength of Ti-Si-C occurs and both materials maintain moderate strength at higher irradiation conditions. Microscopy and compilation of properties of $M_{n+1}AX_n$ (MAX) materials will continue. Additionally, specimens from irradiations to ~6 and ~10 dpa are waiting for activity decay (cooling) before evaluation.

Acknowledgements

The authors would like to thank Patricia Tedder, Brian Eckhart, Bill Comings, Jordan Couch, Michael McAllister and Felipe Mora. Particular thanks to Kenny Curtis for contamination control and activated materials handling. Research was sponsored by the Office of Fusion Energy Sciences, U.S. Department of Energy, under contract DE-AC05-00OR22725 with UT-Battelle, LLC.

References

[1] 1. M. W. Barsoum, T. Zhen, S. R. Kalidindi, M. Radovic, and A. Murugaiah, "Fully reversible, dislocation-based compressive deformation of Ti3SiC2 to 1 GPa," *Nat Mater,* 2[2] 107-11 (2003).

[2] 2. S. J. Zinkle and L. L. Snead, "Designing Radiation Resistance in Materials for Fusion Energy," *Annual Review of Materials Research,* 44[1] 241-67 (2014).

[3] 3. A. A. Campbell, W. D. Porter, Y. Katoh, and L. L. Snead, "Method for Analyzing Passive Silicon Carbide Thermometry with a Continuous Dilatometer to Determine Irradiation Temperature," *submitted to Journal of Nuclear Materials* (2015).

[4] 4. D. J. Tallman, E. N. Hoffman, E. a. N. Caspi, B. L. Garcia-Diaz, G. Kohse, R. L. Sindelar, and M. W. Barsoum, "Effect of neutron irradiation on select MAX phases," *Acta Mater.,* 85[0] 132-43 (2015).

[5] 5. M. K. Patel, D. J. Tallman, J. A. Valdez, J. Aguiar, O. Anderoglu, M. Tang, J. Griggs, E. G. Fu, Y. Q. Wang, and M. W. Barsoum, "Effect of helium irradiation on Ti3AlC2 at 500 degrees C," *Scr. Mater.,* 77 1-4 (2014).